Spiropyran Modified Micro-fluidic Chip Channels as Photonically Controlled Self-Indicating System for Metal Ion Accumulation and Release

Fernando Benito-Lopez, Silvia Scarmagnani, Zarah Walsh, Brett Paull, Mirek Macka and Dermot Diamond*

National Centre for Sensor research, School of Chemical Sciences, Dublin 9, Ireland

E-mail: fernando.lopez@dcu.ie, silvia.scarmagnani@dcu.ie, zarah.walsh2@mail.dcu.ie, brett.paull@dcu.ie, mirek.macka@dcu.ie, dermot.diamond@dcu.ie

* Author to whom correspondence should be addressed; Tel.: + 00353-1-700 7937; Fax: + 353-1-7007995

Abstract

In this paper, we show how through integrating the beneficial characteristics of micro-fluidic devices and spiropyrans dyes, a simple and very innovative chip configured as an on-line photonically controlled self-indicating system for metal ion accumulation and release can be realised. The micro-fluidic device consists of five independent 94 μm depth, 150 μm width channels fabricated in polydimethylsiloxane. The spiropyran 1'-(3-carboxypropyl)-3,3'-dimethyl-6-nitrospiro-1-benzopyran-2,2'-indoline is immobilised by physical adsorption into a polydimethylsiloxane matrix and covalently on the ozone plasma activated polydimehylsiloxane micro-channel walls. When the colourless, inactive, spiropyran coating absorbs UV light it switches to the highly coloured merocyanine form, which also has an active binding site for certain metal ions. Therefore metal ion uptake can be triggered using UV light and subsequently reversed on demand by shining white light on the coloured complex, which regenerates the inactive spiropyran form, and releases the metal ion. When stock solutions of several metal ions (Ca^{2+}, Zn^{2+}, Hg^{2+}, Cu^{2+}, Co^{2+}) are pumped independently through the five channels, different optical responses were observed for each metal, and the platform can therefore be regarded as a micro-structured device for online self-indicating metal ion complexation, accumulation and release.

Keywords: chip array; micro-fluidic chip; spiropyran; PDMS; metal ion.

1. Introduction

Micro-fluidic chips are particularly attractive in biological and life sciences for analytical purposes because they provide a convenient small platform for rapid analysis and detection [1, 2]. The small characteristic dimensions of micro-fluidic devices result in extremely small internal volumes and high surface-to-volume ratios, which lead to improved heat and mass transfer rates. At this small scale, surface effects become dominant in fluid handling and surface properties play a crucial role in chip-based applications [3].

Furthermore, continuous flow operation facilitates real-time measurements and consequently fast analysis protocols. Additionally, gated micro-channels are individually accessible and addressable platforms. Thus, production of high density probe arrays can be achieved within a single device [4]. Such arrays in principle enable thousands of analyses to be performed simultaneously [5].

Traditionally, the determination of ions has been performed using a number of approaches including optical instrumental methods (*e.g.*, atomic absorption, and inductively-coupled plasma-optical emission or mass spectrometry), "wet" methods, or ion-selective electrodes [6]. These approaches are associated with significant limitations; for example, optical methods tend to have relatively high power demand and large reagent consumption and instrumental apparatus is not portable. Wet methods typically involve time-consuming sample-treatment steps and ISEs suffer from interferences, rapid loss of sensitivity and drift, and consequently require frequent calibration. In considering how to overcome such limitations, micro-fluidic devices emerge as a potential solution to some of these challenges. For example, these devices can integrate complex sample handling processes, calibration, and detection

steps into a compact, portable system. Moreover they require small sample volumes (low μl or nl), consume little power, and are easily constructed for multi-analyte detection, either through multiple parallel fluidic architectures [4] or by using arrays of detection elements [7].

Micro-fluidic devices have been applied in areas such as environmental analysis [8], and medical diagnostics [9], where targets are usually small molecules and ionic species. For instance, in the mentioned areas, tremendous amounts of time, reagent, and sample can be saved by employing micro-fluidic devices to perform multi-analyte or array detection of important species, rather than conventional bench instruments. Furthermore, monitoring can be carried out in real-time at point-of-need, rather than bringing samples back to a centralised facility for subsequent analysis

Organic photochromic compounds like spiropyrans are particularly interesting targets for the development of new approaches to sensing since they offer new routes to multi-functional materials that take advantage of their photo-reversible inter-conversion between two thermodynamically stable states (a spiropyran (SP) form, and a merocyanine (MC) form, see scheme 1, which have dramatically different charge, polarity and molecular conformations [10]. Furthermore, they can be easily incorporated into membranes for improved robustness and ease of handling [11], but from our perspective, most interesting of all, they have metal ion-binding and molecular recognition properties which are only manifested by the MC form [12-19]. Based on the coordination-induced photochromism characteristic of the MC form, spiropyrans have been employed as molecular probes for metal ions and organic molecules [20].

This is illustrated for the 1'-(3-carboxypropyl)-3,3'-dimethyl-6-nitrospiro-1-benzopyran-2,2'-indoline derivative (SP-COOH) in scheme 2. Upon exposure to UV

light, the colourless SP-COOH form switches to the highly coloured MC-COOH form, which can complex certain metal ions such as Cu^{2+} [17] and Co^{2+} [21]. Metal ion complexation is accompanied by characteristic changes in the visible absorbance spectrum or fluorescence emission spectrum. Upon exposure to white light, the inactive SP-COOH form is regenerated, and the metal ion is released.

In this paper, we show that immobilisation of photochromic spiropyran molecules like SP-COOH on the PDMS matrix surrounding the micro-channels, as well as in their surface, confined in a micro-fluidic chip can be used for the fabrication of a photonically controlled self-indicating system for metal ion uptake and release. The micro-channels are functionalised by simply flowing solutions through the channels that had previously been activated by UV/ozone treatment. Using this approach, tedious synthesis, purification steps, and/or complicated immobilisation techniques are unnecessary [22]. The result is a micro-chip, where it is optically possible to observe the binding and release effect of several metal ions with MC-COOH using five independent channels, one metal solution per channel, simultaneously, with a single fluorescence "snapshot".

2. Experimental Section

2.1 Materials and instruments

6-Nitro-19,39,39-trimethylspiro[2H-1]-benzopyran-2,29-indoline 98% (SP), was purchased from Aldrich. The requisite spiropyran handle, 11'-(3-carboxypropyl)-3,3'-dimethyl-6-nitrospiro-[2H-1]-benzopyran-2,2'- indoline (SP-COOH, Scheme 1) was produced in a three-step sequence as described elsewhere [23]. Ethanol anhydrous, Calcium chloride, copper (II) nitrate trihydrate, mercury (II) chloride, zinc chloride, cobalt (II) nitrate hexahydrate were purchased from Sigma Aldrich (Ireland).

UV-Vis spectra were recorded on a UV-Vis-NIR Perkin-Elmer Lambda 900 spectrometer. Fluorescence spectra were recorded with a Perkin-Elmer luminescence spectrometer model LS50B. The UV irradiation source (BONDwand UV-365 nm) was obtained from the Electrolite Corporation. UV/ozone treatment of the PDMS chip surface (6 min UV irradiation followed by 20 min ozone action) was carried out in a commercially available UV/ozone chamber (PSD-UV, Novascan Technologies, Ames, IA, USA). Manufacturer specifications for the 50 W system state that approximately 50 % of the total lamp output power is delivered around the 254 nm peak, and 5 % around the 185 nm peak. The distance between the UV source and the PDMS chips was 4.45 cm for this study. Since the surface energy of the UV/ozone-treated PDMS was a function of storage time [24, 25], all the surface modifications were performed directly after the treatment.

Fluorescence images were processed by a research inverted system microscope (Olympus, IX71, Japan) equipped with an EXFO X-Cite 120 fluorescent light source. UV excitation light (λ = 373 nm)-emission (λ = 456 nm) and a green excitation light (510 nm $\leq \lambda \leq$ 550 nm) was filtered using a DAPI and PI filter cube set). Photomicrographs were taken with a charge coupled device (CCD) Olympus DP70 (12.5 million-pixel cooled digital colour camera) for image acquisition coupled to the inverted microscope, using Cell ^{IM} & Cell ^{IR} image software for life science microscopy (Olympus). Meniscus contact angle measurements of the PDMS microchannel were measured by optical microscopy. The wettability of modified PDMS flat surfaces were measured using a G 2 contact angle goniometer (Krüss GmbH, Germany).

2.2 Preparation of standard solutions for metal ions and spiropyrans

Ethanol was used throughout for the preparation of all solutions. A series of 10^{-2} M standard metal ion solutions, Ca^{2+}, Zn^{2+}, Hg^{2+}, Cu^{2+}, Co^{2+}, were prepared, as were 10^{-3} M SP and SP-COOH solutions. Solutions were filtered before being introduced in the chip to avoid particles, which could clog the chip channels, using in-line microfilter assemblies (M-520, 0.5 mm PEEK™, Microtight®, Upchurch Scientific, Harbor, Washington).

2.3 Micro-fluidic device fabrication

The chips were fabricated by rapid phototyping and replication techniques. The micro-fluidic design was initially generated using a computer CAD drawing package. Following an initial check of the dimensions from a printout, the pattern was transferred onto a transparency (3M, CG3300) using a photocopying machine (HP Laser Jet 4050 series PS, 1200 dpi resolution), with printing repeated three times on the same transparency. This transparency served as a photomask for contact photolithography.

The chips were fabricated in PDMS (Sylgard 184, Farnell, Ireland) using standard micro-fabrication procedures [26]. Briefly, a master was created on a silicon wafer by sequentially spinning on a layer of SU-8 photoresist, 3050, (Microchem, Newton, MA) and exposing to UV light through the mask to polymerise regions that were exposed. After dissolving the unpolymerised photoresist, a positive relief of the channel structure was left on the wafer; this structure acted as a master for casting PDMS channels.

Using the master, a negative relief of the structure on the master was made in PDMS by replica moulding. This involved pouring PDMS prepolymer over the master to form a layer approximately 2 mm thick, curing the polymer at 60 ºC for 1 h,

and peeling it off of the master. The whole process from design to replica took less than 1.5 h. This fabrication technique is less expensive and requires less time for design, fabrication, and testing of new channel configurations than conventional fabrication techniques [27].

The PDMS replica was then irreversibly sealed to a 1.1 mm thick Pyrex glass slide (Super Premium, VWR International) by adhesion after UV/ozone activation of the PDMS surface. The rectangular channel dimensions were 27 mm (length), approximately 150 μm (width), and 94 μm (depth). The inlets and outlets were 1 cm (length), 94 μm (depth) and 170 μm (width) to permit better interconnection with the silica capillary tubing, 150 μm outer diameter (OD), 50 μm inner diameter (ID), (Polymicro Technologies, Composite Metal Services Ltd, Ireland). Silica capillary tubing was inserted in the inlets and outlets of the chip immediately after surface modification and glued using epoxy Araldite 2026 glue (Farnell, Ireland), Figure 1.

2.4 Experimental Set- up

The chip is easily placed in the microscope holder since the base of each chip is a standard 75 x 25 mm microscope slide. Solutions were introduced into the channels through each independent inlet by means of a Harvard microdialysis pump (flow rate 0.1–20 μL min^{-1} using 1 mL syringes, Harvard, apparatus PHD 2000), equipped with a home-made five syringe holder, onto which 100 μL Hamilton syringes were mounted. Syringes were connected to fused silica capillaries by means of NanoTight™ unions and fittings (Upchurch Scientific), Figure 2. The standard metal ion solutions were flushed through the channels at 1 μL min^{-1} and fluorescence emission was recorded 5 min after the channels were completely filled with each solution.

2.5 Micro-fluidic device functionalisation

Immediately after exposure of the PDMS chips to UV/ozone and sealing to the glass slide, the activated channels where filled with a 10^{-3} M solution of SP-COOH in ethanol using a 100 μL Hamilton syringe connected to a silica capillary tubing (150 OD, 50 ID) by means of a NanoTight™ union and fitting. The channels were refilled with fresh solution every minute for 10 minutes. The SP-COOH ethanol solution 10^{-3} M was irradiated with UV light (365 nm) for 1 min before the experiments and thereafter it was kept in the dark, thus ensuring the merocyanine form, MC-COOH, is dominant in the solution.

The chips were then placed in an oven for 2 h at 60 ºC in the dark. This treatment ensures that the PDMS surface recovers its natural hydrophobicity, after UV/ozone treatment and MC-COOH functionalisation. Experimentally was found that the meniscus contact angle values of a PDMS channel that was UV/ozone activated and then placed in the oven for 2 h at 60 ºC in the dark and a PDMS channel without any treatment are the same within the error (α = 173°). After this, the micro-fluidic connections where added to the chips (see section 2.2) and the micro-fluidic devices were flushed for 10 min with ethanol (5 μL min^{-1}, 100 μL syringes, Harvard microdialysis pump) and then sonicated (Branson, 5510) in ethanol for 15 min to eliminate any SP-COOH that is not immobilised/adsorbed after UV/ozone activation.

As blank experiments, the same procedure was followed with two other micro-fluidic devices, in one case using non-carboxylated SP, and in the other, using ethanol only.

3. Results and Discussion

3.1. Characterisation of SP-COOH functionalised PDMS surfaces in micro-fluidic devices

To automate the fabrication of the self-indicating system, a five-channel chip suitable for the parallel immobilisation of photonically controlled spiropyran chromophores under continuous flow was designed. Each channel was individually addressed and functionalised with SP-COOH, Figure 1. Despite the fact that in this work all channels were functionalised with the same spiropyran moiety, it should be appreciated that each of the channels can be modified with a different spiropyran derivative, enabling parallel characterisation and analytical studies to be carried out and so, enhance metal ion selectivity [16, 28]. However, in this work, we have focused only on the SP-COOH derivative and it its metal binding/releasing properties.

The five channels integrated in the chip are 4 mm (length), approximately 150 μm (width), and 94 μm (depth) in the observation zone with 300 μm channel separation. Each channel has an independent inlet and outlet, see experimental section 2.3.

The general protocol for the functionalisation of the five channels with SP-COOH consists of initial activation of the channels surfaces using UV/ozone treatment (6 min UV irradiation followed by 20 min ozone action). During this process, silanol groups are introduced at the surface [24]. Immediately after, the solution of MC-COOH in ethanol was passed through the channels for ten minutes following the procedure described in the experimental section 2.5. The functionalisation time is shorter than the time that PDMS walls require for the complete recovery of their natural hydrophobicity which prevents further MC-COOH absorption. The recovery of PDMS surface hydrophobicity is mainly caused by the gradual coverage of a

permanent silica-like structure with free siloxanes and/or reorientation of polar groups as it was studied by contact angle [29] and Chemical Force Microscopy [25] by Vancso *et al*. SP-COOH, which is mainly in its merocyanine form, is able to penetrate deeply into the activated PDMS walls mainly due to its hydrophilic affinity coupled with its porous nature, which enables small molecules to diffuse into the bulk polymer [30, 31]. After oven treatment for PDMS hydrophobicity recovery (see section 2.5), the channels are cleaned with ethanol and sonicated to eliminate any not covalently bonded or not strongly physically adsorbed SP-COOH.

Furthermore, it is believed that SP-COOH reacts covalently with silanol functionalised surface generated after the UV/ozone treatment [32] since, even after sonication of the channels in ethanol, substantial differences in meniscus contact angles were observed between SP-COOH as it is switched between SP and MC forms. The meniscus contact angles were measured using the same procedure as described elsewhere [4]. Figure 3 shows microscopy images of a channel after each functionalisation step. Meniscus contact angles of ca. 173°, 149°, 165° and 174º measured in ethanol inside the micro-channels and contact angles of ca. 106°, 86°, 88° and 98° (± 2°) measured in PDMS flat surfaces, water drop, were found for the hydrophobic PDMS surface, the more hydrophilic UV/ozone activated PDMS surface, the SP-COOH functionalised channels after UV light irradiation and the SP-COOH functionalised after green light irradiation, respectively. After PDMS curing and channel fabrication, the activated surface is highly hydrophobic as a result of the closely packed methyl groups at the surface [33]. When UV/ozone exposition of the PDMS takes place, the surface becomes more hydrophilic reducing significantly the contact angle values. The meniscus contact angle values were measured in the five channels of three independent chips. Standard deviations were typically ca. ± 2°.

The SP-COOH modified channel walls were characterised by contact angle measurements. The contact angle of unmodified PDMS was originally 106°. After MC-COOH surface modification and UV light irradiation, the contact angle decreased to a value of 88°, more hydrophilic, since the MC-COOH form is highly polar and hydrophilic. When irradiated with green light, the MC-COOH returns to its closed not polar spiropyran form 98°, which is less hydrophilic, giving rise to a contact angle value closer to the unmodified PDMS. Thus, the results from this preliminary experiment show that the modification of the micro-channels with the desired sensing spiropyran has been successfully realised.

3.2. Switching properties of the SP-COOH modified PDMS chip walls

When the colourless SP-COOH is illuminated with UV light (350 nm) the chip channels become pink-coloured, and the colour change is easily seen by eye. This effect has been intensively investigated by us using other polymeric surfaces like PMMA [11, 21, 34, 35] and in polystyrene and silica beads [36] where spiropyran derivatives were covalently immobilised. These innovative materials were reversibly switched between the colourless inactive SP form and the highly coloured MC form using low power light sources, such as light emitting diodes (LEDs).

The channels, filled with ethanol, were irradiated with 350 nm UV light for 1 min to convert the SP-COOH to the MC-COOH form. Then, the channels were illuminated with green excitation light, (450-650 nm) for 30 seconds, with fluorescence images being taken every 3 seconds ($\lambda > 590$ nm) [37]. It should be noted that in addition to providing excitation or the fluorescence emission measurements, green light is known to revert the merocyanine form back to the spiropyran form. The decrease in fluorescence intensity of the chip channel walls was

measured *versus* time until fluorescence returns to background levels. The fluorescence emission profiles were normalised by setting the background signal to 0.

Green light exhibits fast and efficient MC→SP switching, reaching full conversion of the whole channel wall region (2 mm thick) in less than 30 s (Figure 4a). It was previously demonstrated that the green region is most effective for the back-conversion of MC to the SP form [21]. The first order rate constant, with a value of 0.51 ± 0.05 s^{-1}, was estimated by fitting the fluorescence intensity decrease over time using Microsoft Excel Solver [34, 38] using the following equation:

$$y = ae^{-kt} + b \quad (1)$$

where y is the normalised fluorescence intensity, a is the normalised fluorescence intensity at time 0, k is the rate constant (s^{-1}) and b is the asymptotic value.

This value is much higher than in previous studies using silica beads functionalised with SP-COOH, [36] 4.8×10^{-5} s^{-1} and slightly higher than the rate constant of spiropyran-doped polystyrene, [34] 10^{-2} s^{-1} in which SP-COOH was entrapped within a polymer layer similar to that employed in this work; using similar light doses. These results clearly imply that the PDMS polymer matrix promotes ring-closing mechanism of MC-COOH to SP-COOH conversion.

Another issue to be considered when dealing with spiropyran photochromic dyes is their photostability over time, as a well documented photobleaching process [39-42] occurs when SP is exposed to UV-Vis radiation for extended time periods. After 10 switching cycles, the efficiency was found to be relatively constant in four different chip positions for two different chips. Figure 4b shows typical results obtained in these experiments for one location on one of these chips. The $\overline{\Delta I}_{SP \to MC} = 235 \pm 18$ *u.a.* and the $\overline{\Delta I}_{MC \to SP} = -237 \pm 21$ *u.a.* for 10 cycles have similar

differences in intensity values, showing that these cycles are reproducible and repeatable, with no hysteresis. This result demonstrates that the micro-fluidic device could be used at least ten times, without significant photobleaching.

3.3. Fluorescence Emission Measurements Associated with SP-COOH Modified PDMS Channel Walls in the Presence of Metal Ions

Spiropyran functionalised micro-channels offer interesting possibilities for controlling metal ion uptake using light, as only the MC form binds with metal ions since the phenolate group of the MC form exhibits ion-binding behaviour, particularly for heavy metals [13, 14, 43, 44]. Moreover, plenty of carboxylic groups of SP-COOH remain free for extra coordination, enhancing the ion-binding behaviour.

Therefore it should be possible to determine when and where ion binding occurs within a channel (*e.g.* by illuminating with a UV light), while ion release can be similarly controlled by illumination with green light. In addition, once the PDMS walls with SP-COOH are reconverted the MC form, the surface is ready for re-use. Furthermore, the system is inherently self-indicating, and by monitoring the fluorescence, it can be seen which form is present (SP or MC) and whether ions are bound (fluorescence profile of the channel, Figure 5a). In Figure 5b a schematic representation of a chip channel shows where the SP-COOH in its MC-COOH form is physisorbed inside the PDMS channel walls with the lines indicating the locations where experiments were carried out.

It has been previously demonstrated that the interaction of metal ions with the fluorescent merocyanine form may induce [17, 45] quenching or enhancement of the fluorescence emission.

Based on previous solution studies, Ca^{2+} [36], Zn^{2+} [13], Hg^{2+} [14], Cu^{2+} [17, 28], Co^{2+}[21] ions were chosen to investigate self-indicating complex formation. When the MC-COOH-activated channel walls are placed in contact with the different metal solutions, the fluorescence emission varies with each metal ion, see Figure 5c. The emission change is reversible, as upon irradiation with green light and filling the channels with fresh solvent, the SP-COOH form is restored and the metal ion is expelled. Furthermore the channels can be converted back to the MC-COOH form ready for another ion binding cycle using UV light.

These changes can be monitored by recording the fluorescence emission intensity (λ = 590 nm) of the channels in the presence of metal ion solutions and comparing to the emission in pure ethanol, Figure 5c. These observed changes in intensity are reproducible for each of the metals even using different micro-fluidic devices and channel positions. It should be taken into account that all these processes are performed under continuous flow conditions using an externally controlled syringe pump. For instance, in the presence of Co^{2+}, Ca^{2+} or Cu^{2+} ions, the fluorescence is quenched substantially by -77, -30 and -27 %, respectively (relative fluorescence intensity), while in the case of Zn^{2+} almost no fluorescence change was observed. In the other hand, a significant increase in fluorescence intensity occurs in the presence of Hg^{2+} ions. These intensity changes are associated with characteristic shifts and intensity reduction/increase in the fluorescence and UV-Vis spectrum peak at λ= 605 nm (fluorescence) and at λ = 531 nm (UV-Vis) when metal ion complex with merocyanine. Figure 6 shows all the fluorescence spectra and two UV-Vis spectra for the five metals coordinated with MC-COOH in solution. It can be observed that the relative fluorescence intensity of the complex MC-COOH-M^{2+} varies with respect to the values obtained in the micro-fluidic device showed in Figure 5c. For instance,

MC-COOH-Hg^{2+} relative fluorescence intensity increases approximately 42 % in solution while only 30 % in the micro-fluidic device. The other values in solution are for Co^{2+} a 92 %, for Ca^{2+} a 82 % for Cu^{2+} a 78 % and for Zn^{2+} only a 6 % quenching of relative fluorescence intensity and also these values differ slightly form the micro-fluidic device experiments. The reason for that can be attributed to the different environment where complexation takes place, in ethanol solution, Figure 6, or in the PDMS matrix and surface, Figure 5c. In the ethanol solution all the MC-COOH molecules are available for complexation with the metal ions while in the PDMS, matrix may interfere during metal complexation.

In Figure 6a the fluorescence spectrum of the protonated MC-COOH form is shown with a λ_{max} = 553 nm for clarification, indicating that the MC-COOH-H^+ is not present at this experimental conditions.

Figure 7 shows three snap shots of three channels in one micro-fluidic device and their respective fluorescence intensity profiles before and after three consecutive capture/release metal ion experiments (Ca^{2+}). The channels were pre-filled with ethanol and UV light irradiated to generate the MC-COOH form (I_0 = 280 a.u.). Upon flushing with Ca^{2+} loaded ethanol solution (following the same procedure described above) complexation of the metal ions occurs and is directly indicated by a substantial decrease in fluorescence emission intensity (I = 180 a.u.). Subsequently, upon exposure to green light, the Ca^{2+} is released and the original fluorescence intensity is recovered again (I_0 = 280 a.u.). This experiment was successfully repeated three times. As can be appreciated from Figure 7, the fluorescence intensity before the experiments (photo-1) is comparable with the one after the three consecutive capture/release metal ion complexation experiments (photo-3); suggesting that the

system is stable and the obtained data are reproducible and comparable for each experiment.

As blank experiments, a micro-fluidic device functionalised with non-carboxylated spiropyran (SP) was also fabricated following the same procedure described above Figure 8, see experimental section 2.5. The fluorescence of the PDMS after fabrication is negligible (photo-1, I_0 = 30 a.u.), and decreases to zero after first experiment with the Cu^{2+} ion solution (photo-2). This experiment shows that for fabricating a stable sensing PDMS chip, the carboxylic chain of the SP-COOH is necessary as it appears to stabilise the whole molecule inside the hydrophobic porous PDMS polymeric network [46]. A third PDMS micro-reactor (non-functionalised) was also tested for fluorescence and did not exhibit any inherent fluorescence under the conditions employed in these investigations.

4. Conclusions

The results presented here show that an array of micro-channels in a PDMS chip can be fabricated and subsequently functionalised with photochromic spiropyran (SP-COOH). Upon exposure to appropriate stimuli, this platform displays photo-controlled uptake and release of certain metal ions, and examination of fluorescence emission can provide evidence of which ions are present. This behaviour is fully reversible through multiple cycles. In addition, the platform is inexpensive, and can be made using relatively simple equipment.

This presents a model system of a micro-fluidic detector based on a photoswitchable/photochromic fluorescent dye, which could be coupled with an additional selective stage (e.g. selective reagent or a micro-separation column) to give

a platform capable of accumulating/release a number of metal ions, and this is a direction this research will be taken in the future.

5. Acknowledgements

The project has been carried out with the support of the Irish Research Council for Science, Engineering and Technology (IRCSET) fellowship number 2089 and Science Foundation Ireland under the under Grants No. 03/IN3/1361 (Adaptive Information Cluster) and 07/RPF/MASF812.

6. References and Notes

1. J. West, M. Becker, S. Tombrink, A. Manz, Micro Total Analysis Systems: Latest Achievements. Anal. Chem. (2008), 80, 4403-4419.

2. P. Yager, T. Edwards, E. Fu, K. Helton, K. Nelson, M.R. Tam, B.H. Weigl, Microfluidic Diagnostic Technologies for Global Public Health. Nature (2006), 442, 412-418.

3. S.H. Kim, Y. Yang, M. Kim, S.W. Nam, K.M. Lee, N.Y. Lee, Y.S. Kim, S. Park, Simple Route to Hydrophilic Microfluidic Chip Fabrication Using an Ultraviolet (Uv)-Cured Polymer. Adv. Funct. Mater. (2007), 17, 3493-3498.

4. L. Basabe-Desmonts, F. Benito-Lopez, H. Gardeniers, R. Duwel, A. van den Berg, D.N. Reinhoudt, M. Crego-Calama, Fluorescent Sensor Array in a Microfluidic Chip. Anal. Bioanal. Chem. (2008), 390, 307-315.

5. L. Dong, A.K. Agarwal, D.J. Beebe, H.R. Jiang, Adaptive Liquid Microlenses Activated by Stimuli-Responsive Hydrogels. Nature (2006), 442, 551-554.

6. R.D. Johnson, V.G. Gaualas, S. Daunert, L.G. Bachas, Microfluidic Ion-Sensing Devices. Anal. Chim. Acta (2008), 613, 20-30.

7. T.S. Dalavoy, D.P. Wernette, M.J. Gong, J.V. Sweedler, Y. Lu, B.R. Flachsbart, M.A. Shannon, P.W. Bohn, D.M. Cropek, Immobilization of Dnazyme Catalytic Beacons on PMMA for Pb2+ Detection. Lab Chip (2008), 8, 786-793.

8. A. Bowden, D. Diamond, The Determination of Phosphorus in a Microfluidic Manifold Demonstrating Long-Term Reagent Lifetime and Chemical Stability Utilising a Colorimetric Method. Sens. Actuators, B (2003), 90, 170-174.

9. C. Joensson, M. Aronsson, G. Rundstroem, C. Pettersson, I. Mendel-Hartvig, J. Bakker, E. Martinsson, B. Liedberg, B. MacCraith, O. Oehman, J. Melin, Silane-Dextran Chemistry on Lateral Flow Polymer Chips for Immunoassays. Lab Chip (2008), 8, 1191-1197.

10. H. Tian, Y.L. Feng, Next Step of Photochromic Switches? J. Mater. Chem. (2008), 18, 1617-1622.

11. A. Radu, S. Scarmagnani, R. Byrne, C. Slater, K.T. Lau, D. Diamond, Photonic Modulation of Surface Properties: A Novel Concept in Chemical Sensing. J. Phys. D: Appl. Phys. (2007), 40, 7238-7244.

12. M.S. Attia, M.M.H. Khalil, M.S.A. Abdel-Mottaleb, M.B. Lukyanova, Y.A. Alekseenko, B. Lukyanov, Effect of Complexation with Lanthanide Metal Ions on the Photochromism of (1,3,3-Trimethyl-5 '-Hydroxy-6 '-Formyl-Indoline-Spiro2,2 '-[2h]Chromene) in Different Media. Int. J. Photoenergy (2006).

13. G.E. Collins, L.S. Choi, K.J. Ewing, V. Michelet, C.M. Bowen, J.D. Winkler, Photoinduced Switching of Metal Complexation by Quinolinospiropyranindolines in Polar Solvents. Chem. Commun. (1999), 321-322.

14. L. Evans, G.E. Collins, R.E. Shaffer, V. Michelet, J.D. Winkler, Selective Metals Determination with a Photoreversible Spirobenzopyran. Anal. Chem. (1999), 71, 5322-5327.

15. J.Q. Ren, H. Tian, Thermally Stable Merocyanine Form of Photochromic Spiropyran with Aluminum Ion as a Reversible Photo-Driven Sensor in Aqueous Solution. Sensors (2007), 7, 3166-3178.

16. Y. Zhang, N. Shao, R.H. Yang, K.A. Li, F. Liu, W.H. Chan, T. Mo, Utilization of a Spiropyran Derivative in a Polymeric Film Optode for Selective Fluorescent Sensing of Zinc Ion. Sci. China, Ser. B Chem. (2006), 49, 246-255.

17. N. Shao, J.Y. Jin, H. Wang, Y. Zhang, R.H. Yang, W.H. Chan, Tunable Photochromism of Spirobenzopyran Via Selective Metal Ion Coordination: An Efficient Visula and Ratioing Fluorescent Probe for Divalent Copper Ion. Anal. Chem. (2008), 80, 3466-3475.

18. T. Suzuki, T. Kato, H. Shinozaki, Photo-Reversible Pb2+-Complexation of Thermosensitive Poly(N-Isopropyl Acrylamide-Co-Spiropyran Acrylate) in Water. Chem. Commun. (2004), 2036-2037.

19. H. Wu, D.Q. Zhang, L. Su, K. Ohkubo, C.X. Zhang, S.W. Yin, L.Q. Mao, Z.G. Shuai, S. Fukuzumi, D.B. Zhu, Intramolecular Electron Transfer within the Substituted Tetrathiafulvalene-Quinone Dyads: Facilitated by Metal Ion and Photomodulation in the Presence of Spiropyran. J. Am. Chem. Soc. (2007), 129, 6839-6846.

20. M. Inouye, Artificial-Signaling Receptors for Biologically Important Chemical Species. Coord. Chem. Rev. (1996), 148, 265-283.

21. R.J. Byrne, S.E. Stitzel, D. Diamond, Photo-Regenerable Surface with Potential for Optical Sensing. J. Mater. Chem. (2006), 16, 1332-1337.

22. M.H. Yang, M.C. Biewer, Monitoring Surface Reactions Optically in a Self-Assembled Monolayer with a Photochromic Core. Tetrahedron Lett. (2005), 46, 349-351.

23. A.A. Garcia, S. Cherian, J. Park, D. Gust, F. Jahnke, R. Rosario, Photon-Controlled Phase Partitioning of Spiropyrans. J. Phys. Chem. A (2000), 104, 6103-6107.

24. J. Song, J.F.L. Duval, M.A.C. Stuart, H. Hillborg, U. Gunst, H.F. Arlinghaus, G.J. Vancso, Surface Ionization State and Nanoscale Chemical Composition of Uv-Irradiated Poly(Dimethylsiloxane) Probed by Chemical Force Microscopy, Force Titration, and Electrokinetic Measurements. Langmuir (2007), 23, 5430-5438.

25. H. Hillborg, N. Tomczak, A. Olah, H. Schonherr, G.J. Vancso, Nanoscale Hydrophobic Recovery: A Chemical Force Microscopy Study of Uv/Ozone-Treated Cross-Linked Poly(Dimethylsiloxane). Langmuir (2004), 20, 785-794.

26. D.C. Duffy, J.C. McDonald, O.J.A. Schueller, G.M. Whitesides, Rapid Prototyping of Microfluidic Systems in Poly(Dimethylsiloxane). Anal. Chem. (1998), 70, 4974-4984.

27. J.M.K. Ng, I. Gitlin, A.D. Stroock, G.M. Whitesides, Components for Integrated Poly(Dimethylsiloxane) Microfluidic Systems. Electrophoresis (2002), 23, 3461-3473.

28. N. Shao, Y. Zhang, S.M. Cheung, R.H. Yang, W.H. Chan, T. Mo, K.A. Li, F. Liu, Copper Ion-Selective Fluorescent Sensor Based on the Inner Filter Effect Using a Spiropyran Derivative. Anal. Chem. (2005), 77, 7294-7303.

29. A. Olah, H. Hillborg, G.J. Vancso, Hydrophobic Recovery of Uv/Ozone Treated Poly(Dimethylsiloxane): Adhesion Studies by Contact Mechanics and Mechanism of Surface Modification. Appl. Surf. Sci. (2005), 239, 410-423.

30. E. Baltussen, P. Sandra, F. David, C. Cramers, Stir Bar Sorptive Extraction (Sbse), a Novel Extraction Technique for Aqueous Samples: Theory and Principles. J. Microcolumn Sep. (1999), 11, 737-747.

31. G. Theodoridis, M.A. Lontou, F. Michopoulos, M. Sucha, T. Gondova, Study of Multiple Solid-Phase Microextraction Combined Off-Line with High Performance Liquid Chromatography - Application in the Analysis of Pharmaceuticals in Urine. Anal. Chim. Acta (2004), 516, 197-204.

32. R.P. Young, Infrared Spectroscopic Studies of Adsorption and Catalysis .3. Carboxylic Acids and Their Derivatives Adsorbed on Silica. Can. J. Chem. (1969), 47, 2237-&.

33. M.J. Owen, *Siilicon-Based Polymer Science, a Comprehensive Resource*. Ziegler, J. Fearon, F. W. G.; American Chemical Society: Washington DC, 1990.

34. S. Stitzel, R. Byrne, D. Diamond, Led Switching of Spiropyran-Doped Polymer Films. J. Mater. Sci. (2006), 41, 5841-5844.

35. R. Byrne, D. Diamond, Chemo/Bio-Sensor Networks. Nat. Mater. (2006), 5, 421-424.

36. S. Scarmagnani, Z. Walsh, C. Slater, N. Alhashimy, B. Paull, M. Macka, D. Diamond, Polystyrene Bead-Based System for Optical Sensing Using Spiropyran Photoswitches. J. Mater. Chem. (2008), 18, 5063-5071.

37. R. Rosario, D. Gust, M. Hayes, F. Jahnke, J. Springer, A.A. Garcia, Photon-Modulated Wettability Changes on Spiropyran-Coated Surfaces. Langmuir (2002), 18, 8062-8069.

38. D. Diamond, V.C.A. Hanratty, *Spreadsheet Applications in Chemistry Using Microsoft Excel*. Wiley: New York, 1997.

39. G. Baillet, G. Giusti, R. Guglielmetti, Comparative Photodegradation Study between Spiro[Indoline Oxazine] and Spiro[Indoline Pyran] Derivatives in Solution. J. Photochem. Photobiol., A (1993), 70, 157-161.

40. G. Baillet, M. Campredon, R. Guglielmetti, G. Giusti, C. Aubert, Dealkylation of N-Substituted Indolinospironaphthoxazine Photochromic Compounds under Uv Irradiation. J. Photochem. Photobiol., A (1994), 83, 147-151.

41. R. Matsushima, M. Nishiyama, M. Doi, Improvements in the Fatigue Resistances of Photochromic Compounds. J. Photochem. Photobiol., A (2001), 139, 63-69.

42. R. Demadrille, A. Rabourdin, M. Campredon, G. Giusti, Spectroscopic Characterisation and Photodegradation Studies of Photochromic Spiro[Fluorene-9,3 '-[3 ' H]-Naphtho[2,1-B]Pyrans]. J. Photochem. Photobiol., A (2004), 168, 143-152.

43. A.K. Chibisov, H. Gorner, Complexes of Spiropyran-Derived Merocyanines with Metal Ions: Relaxation Kinetics, Photochemistry and Solvent Effects. Chem. Phys. (1998), 237, 425-442.

44. H. Gorner, A.K. Chibisov, Complexes of Spiropyran-Derived Merocyanines with Metal Ions - Thermally Activated and Light-Induced Processes. J. Chem. Soc., Faraday Trans. (1998), 94, 2557-2564.

45. T. Sakata, D.K. Jackson, S. Mao, G. Marriott, Optically Switchable Chelates: Optical Control and Sensing of Metal Ions. J. Org. Chem. (2008), 73, 227-233.

46. M.W. Toepke, D.J. Beebe, Pdms Absorption of Small Molecules and Consequences in Microfluidic Applications. Lab Chip (2006), 6, 1484-1486.

Scheme 1. Structures of spiropyran (closed), left, and merocyanine (open), right.

Scheme 2. Chemical structure of SP-COOH and MC-COOH and the photoreversible equilibria and metal complexation of the spiropyran SP-COOH with divalent metal ions, SP-COOH-M^{2+}.

Figure 1. PDMS/glass hybrid micro-fluidic device (3.5 x 1.5 cm); **1** and **2** are the inlets and outlets respectively, **3** is the observation area.

Figure 2. Schematic view of the set-up used during measurements.

Figure 3. Optical microscopy images of the ethanol meniscus inside the channel after each functionalisation step of the chip and the contact angle measurement (water drop) of the functionalised PDMS flat surfaces.

Figure 4. (a) Channel wall fluorescence decreases while green light irradiation is applied. **(b)** Fluorescence plotted from the channel walls during switching, n = 10.

Figure 5. a) Fluorescence intensity of the MC-COOH form adsorbed in the PDMS channel walls in the presence of 10^{-3} M cobalt (II) metal ion solution in ethanol (MC-COOH-M^{2+}), (***I***) and fluorescence intensity of the MC-COOH form adsorbed in the PDMS channels walls in ethanol, (I_0). **b)** Schematic representation of a chip channel showing the MC-COOH form physisorbed inside the PDMS channel walls; lines represent the location where experiments were carried out. **c)** Relative fluorescence intensity of the PDMS channel walls in the presence of different 10^{-3} M metal ion solutions in ethanol. The experiment has been repeated three times and the fluorescence intensity error is in the range of ± 10 a.u.

Figure 6. **a)** Fluorescence spectra of MC-COOH (0.25×10^{-3} M) in ethanol, MC-COOH-M^{2+} complexes (1:2) in ethanol [21] and spectrum of protonated MC-COOH-H^{+} (λ_{max} = 553 nm) **b)** UV-Vis spectra of MC-COOH (0.25×10^{-3} M) in ethanol and MC-COOH-M^{2+} complexes (1:2) in ethanol.

Figure 7. Fluorescence intensity images (4x microscope magnification) of the MC-COOH form adsorbed in the PDMS channel walls before (photo-1) and after (photo-3) three consecutive capture/release metal ion experiments (Ca^{2+}) in ethanol and their fluorescence emission intensity profiles. A dotted line across the chip in photos-1, 2 and 3 shows were the fluorescence emission intensity values were taken.

Figure 8. Fluorescence intensity images (4x microscope magnification) of the MC form of non-carboxylated SP adsorbed in the PDMS channel walls before (photo-1) and after (photo-2) one capture/release metal ion experiments in ethanol (Cu^{2+}) and their fluorescence intensity profiles. A dotted line across the chip in photos-1 and 2 shows were the fluorescence emission intensity values.

Scheme 1.

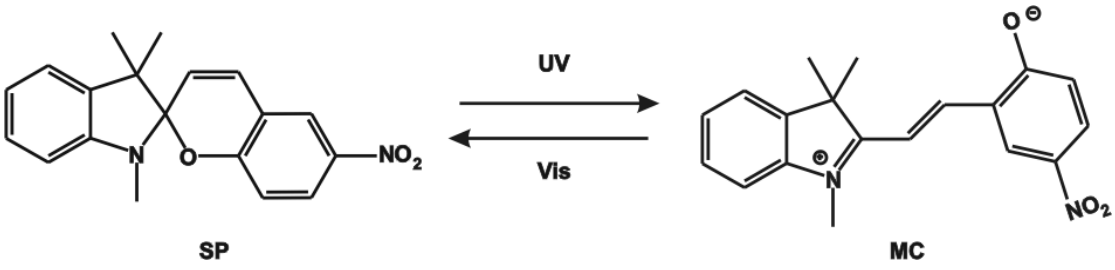

Scheme 2.

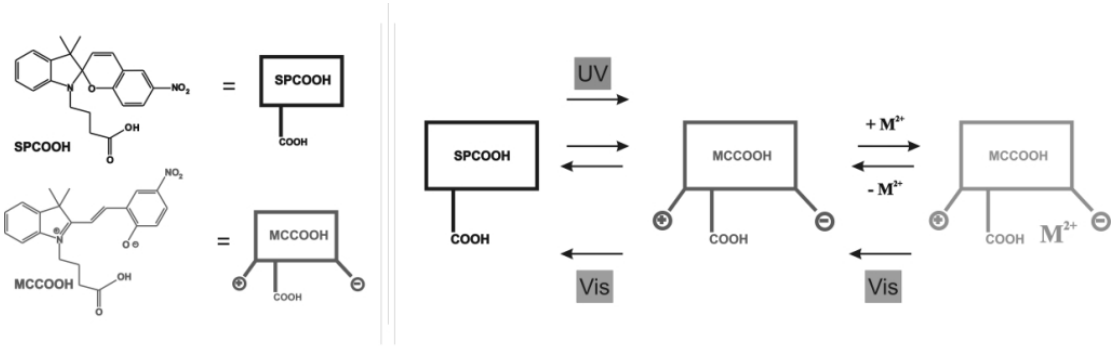

Figure 1.

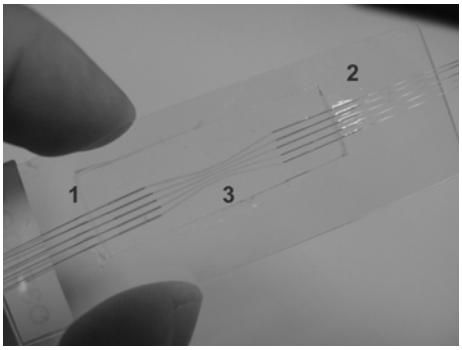

Figure 2.

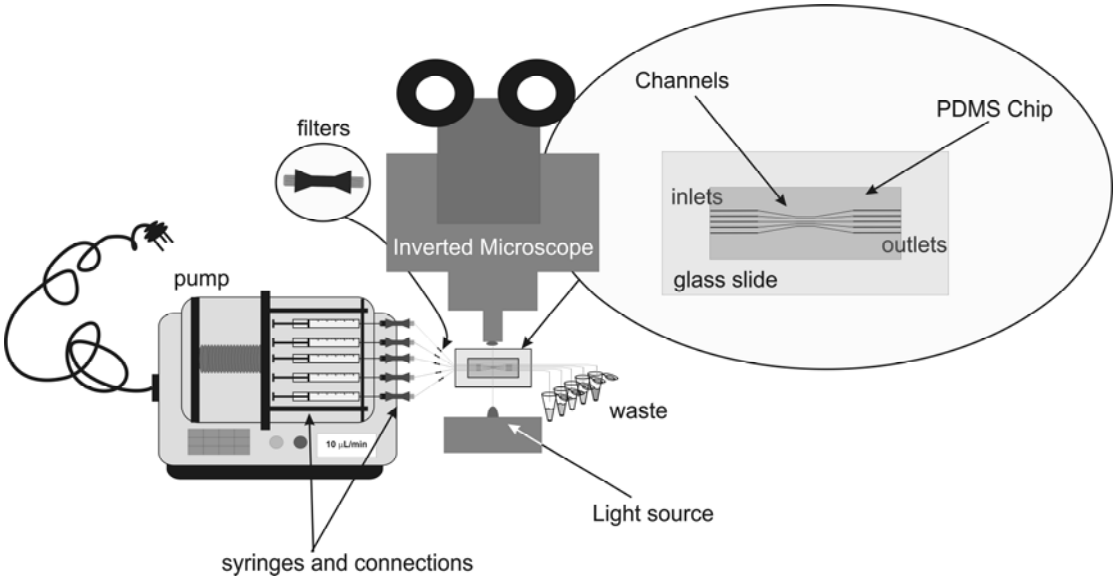

Figure 3.

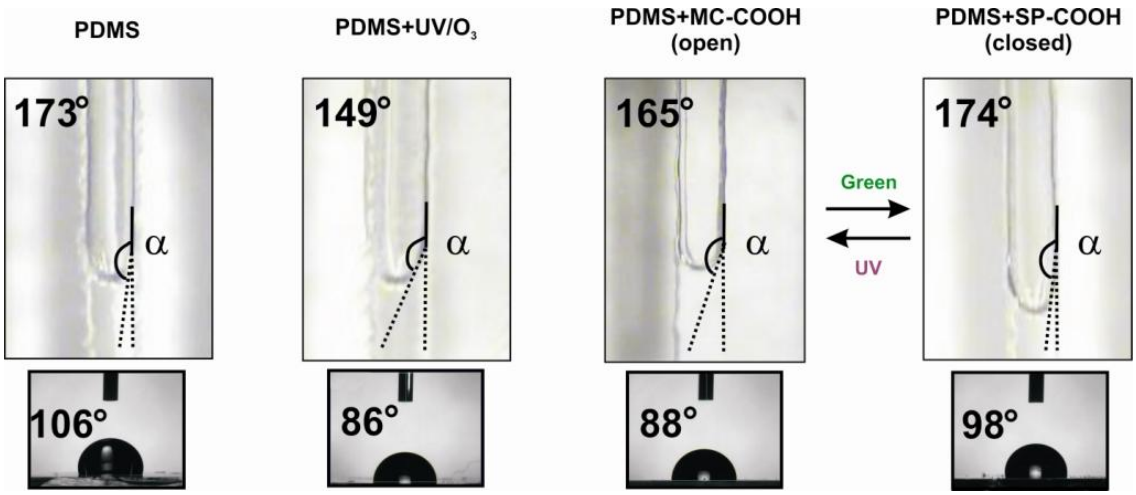

Figure 4.

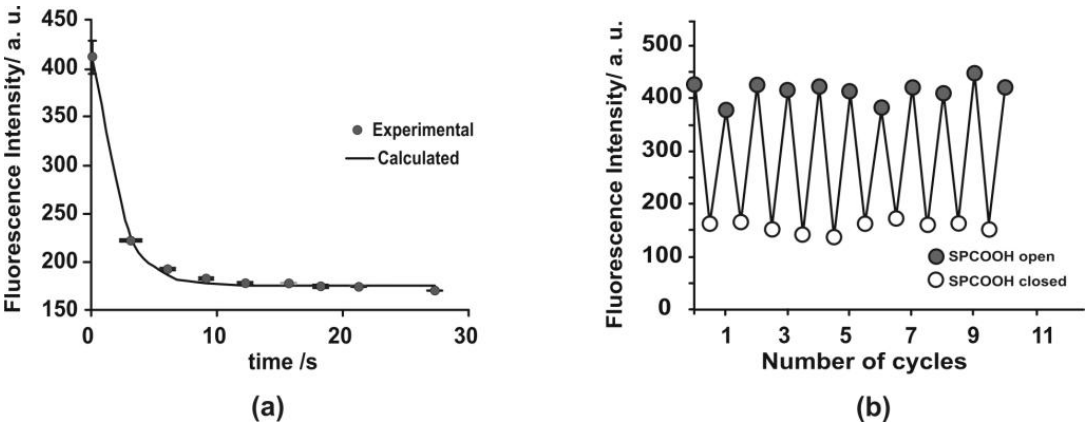

Figure 5.

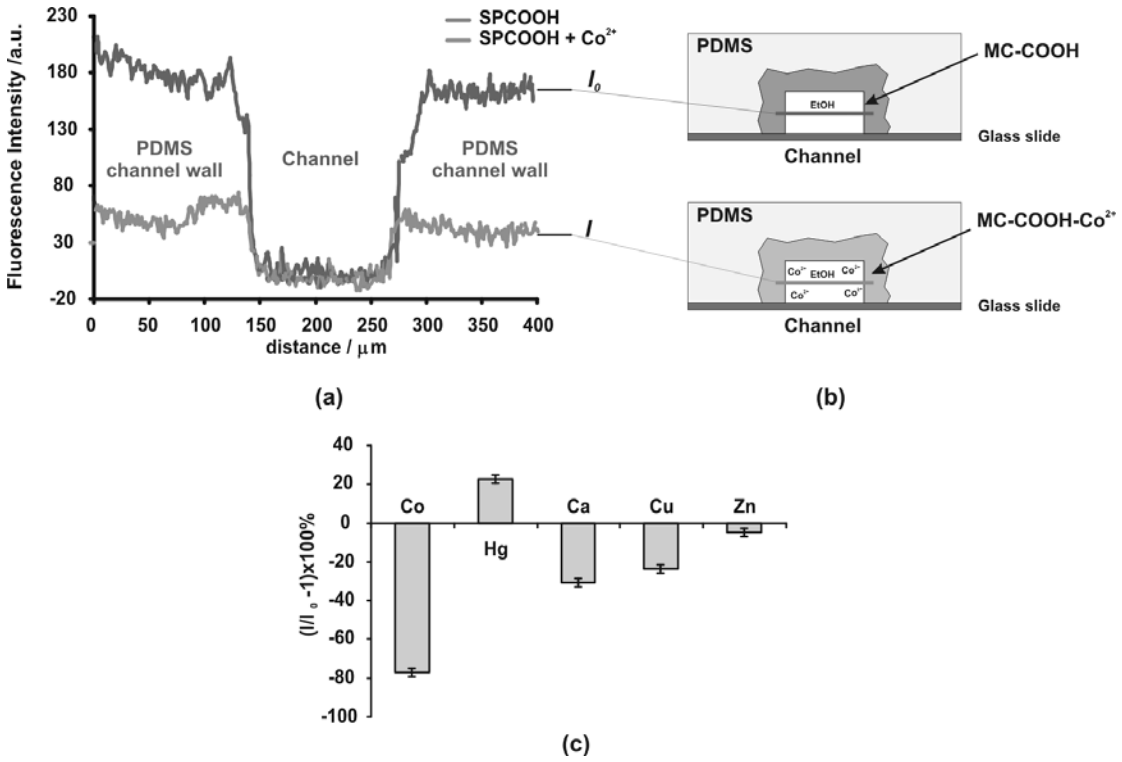

Figure 6.

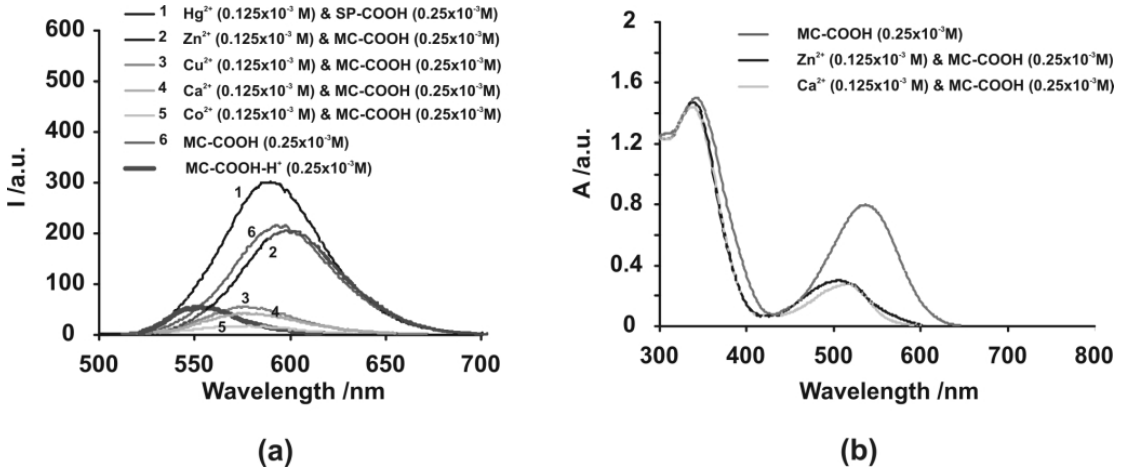

Figure 7.

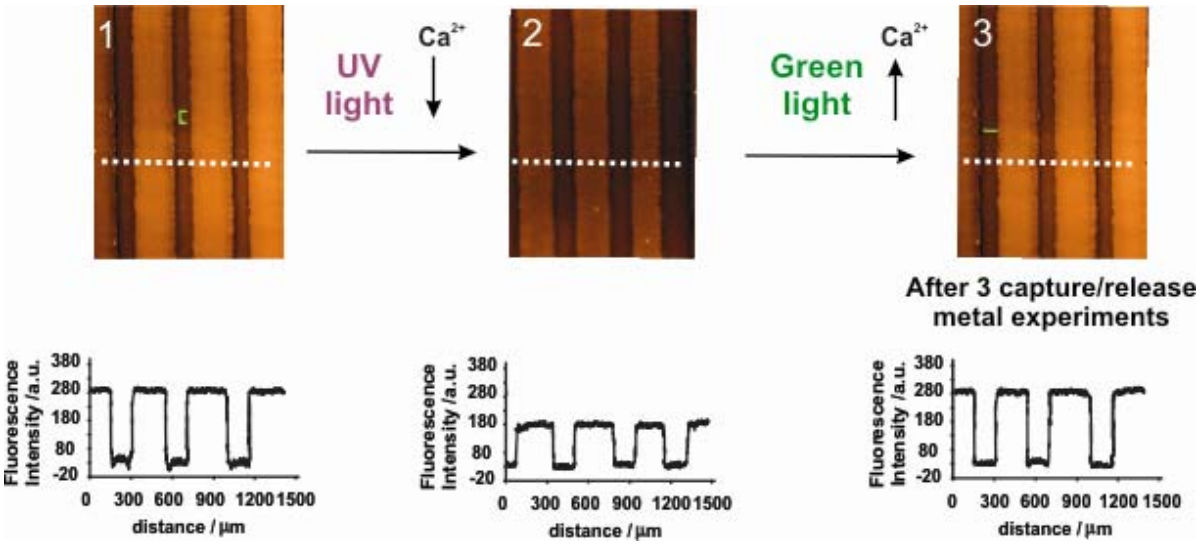
1
UV light
Ca2+
2
Green light
Ca2+
3
After 3 capture/release metal experiments
Fluorescence Intensity /a.u.
380
280
180
80
-20
0 300 600 900 1200 1500
distance / µm

Figure 8.

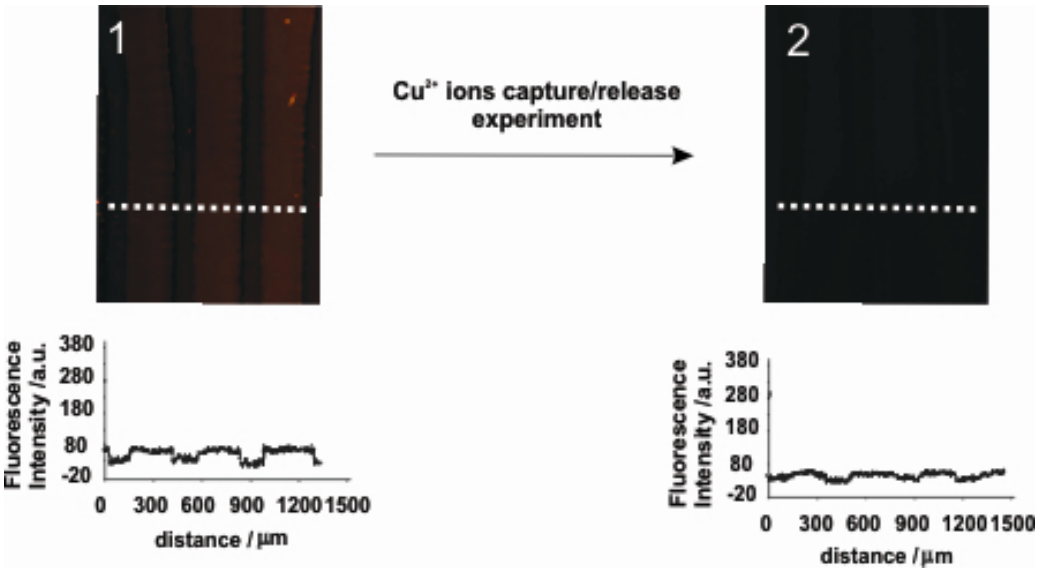
1
Cu2+ ions capture/release experiment
2
Fluorescence Intensity /a.u.
380
280
180
80
-20
0 300 600 900 1200 1500
distance / µm